A review of directional modulation technology

A Review of Directional Modulation Technology

Yuan Ding, Vincent Fusco

The ECIT Institute Queens University of Belfast, Belfast, BT3 9DT, United Kingdom.

Directional modulation (DM) is an emerging technology for securing wireless communications at the physical layer. This promising technology, unlike the conventional key-based cryptographic methods and the key-based physical layer security approaches, locks information signals without any requirements of keys. The locked information can only be fully recovered by the legitimate receiver(s) priory known by DM transmitters. This paper reviews the origin of the DM concept and, particularly, its development in recent years, including its mathematical model, assessment metrics, synthesis approaches, physical realizations, and finally its potential aspects for future studies.

Corresponding author: Yuan Ding; email: yding03@qub.ac.uk; phone: +44 (0)2890 971 806

I. Introduction

Besides connectivity another important factor for modern communication systems is security. Compared with wire-line communication, the security problem is more severe for wireless systems, due to the lack of a physical boundary associated with the broadcasting nature of wireless transmission. This makes confidential information transmitted wirelessly highly vulnerable to interception [1].

Conventionally key-based cryptographic technologies are employed at the higher protocol layers, regardless whether the communication systems is wired or wireless, in order to secure data transmission [2–4]. However, these state-of-the-art encryption algorithms, deemed secure enough nowadays, may eventually be compromised due to ever intense computational resource availability. In order to gain the most fundamental level of security, i.e., information theoretical security, [5], encryption has to be performed at the physical layer, where the raw interchange between bits of information and modulated signal waveforms takes place.

One way to achieve this is to generate keys at the physical layer by exploiting common randomness at the physical layer, e.g., electromagnetic propagation in a reciprocal multipath environment, instead of using mathematical means. However, this security key establishment method, normally involving five critical procedures of channel probing, signal pre-processing, quantization, information reconciliation, and privacy amplification [6], is highly dependent on the characteristics of wireless channels [7, 8], such as multipath and temporal variation. This makes the key generation approach unsuitable for channel invariant-quasi-static and/or line of sight communication environment. Another less complex approach that can be deployed in any

wireless channel scenarios does not involve any keys, i.e., keyless physical layer security [9]. One promising concept of directional modulation (DM), mainly for free space wireless communication, falls into this category, and is the focus of this review paper [10–26].

Generally speaking, DM is a transmitter side technology that is capable of projecting digitally modulated information signals into a pre-specified secure communication spatial direction in free space while simultaneously distorting the constellation formats of the same signals in all other directions, in such a fashion to lower the possibility of interception [11].

Taking as an example a DM system modulated for quadrature phase-shift keying (QPSK), Fig. 1, the standard formatted QPSK constellation patterns, i.e., central-symmetric square in In-phase and Quadrature (IQ) space, are not preserved away from an a-priori defined observation direction θ_0. The fact that the spatial-dependent modulation formats are scrambled along all directions other than θ_0 imposes great challenges on potential eavesdroppers of interception. The DM system models, i.e., the mechanism of constellation pattern distortion, the effectiveness of distortion in terms of security, synthesis approaches, and system demonstrators are discussed in this review paper.

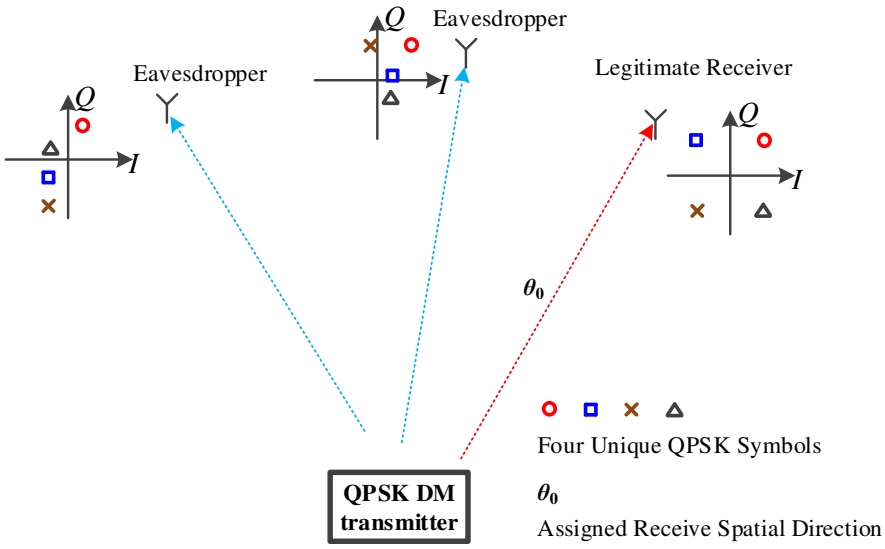

Fig. 1. Illustration of the major properties of a QPSK DM system. Along a pre-specified direction θ_0 a usable constellation is formed. Away from the desired direction the constellations are scrambled.

The rest of this paper is organized as follows. In Section II a mathematical description of DM systems is derived and vector representations in IQ space are established for DM analysis [10]. With the help of these tools, the necessary conditions for DM arrays are obtained. In Section III another fundamental aspect, i.e., valid metrics to evaluate the performance of DM systems in a way that is consistent and which allows direct comparison between different DM systems, is discussed and summarized. Section IV and Section V are devoted to the DM synthesis methods and the DM physical demonstrators available, respectively. Finally Section VI concludes the paper and provides some recommendations for potential future development of the DM technology.

II. DM System Mathematical Description and Vector Model

The DM definition presented in Section I gives us a working definition on what DM technology is. In this section a rigorous mathematical description is developed and a vector model is established for DM systems. With these tools, the essence of the DM technology is revealed, and some key concepts are introduced, which form the basis for following sections.

2.1 Essence of DM technology

Proposition: DM characteristics are enabled by updating beam-forming networks, by either analogue or digital means at any stages of transmitters, at the information rate. It was erroneously believed and incorrectly claimed in [18–31] that the DM properties can only be achieved by applying baseband signals directly onto the radio frequency (RF) frontend or antenna structures.

The above statement is explained as below.

The superimposed radiation from a series of radiating antenna elements in free space, for example the one dimensional (1-D) case, can be formed for N elements, with the summed electric field $\boldsymbol{E}$ at some distant observation point in free space, given as

$$\boldsymbol{E}(\theta) = \frac{e^{-j\vec{k}\cdot\vec{r}}}{|\vec{r}|} \cdot \begin{bmatrix} \boldsymbol{AP}_1(\theta) \\ \boldsymbol{AP}_2(\theta) \\ \mathrm{M} \\ \boldsymbol{AP}_N(\theta) \end{bmatrix}^T \begin{bmatrix} \boldsymbol{A}_1 \cdot e^{j\vec{k}\cdot\vec{x}_1} \\ \boldsymbol{A}_2 \cdot e^{j\vec{k}\cdot\vec{x}_2} \\ \mathrm{M} \\ \boldsymbol{A}_N \cdot e^{j\vec{k}\cdot\vec{x}_N} \end{bmatrix} \tag{1}$$

where $\vec{k}$ is the wavenumber vector along the spatial transmission direction θ, which ranges from 0° to 180° with boresight at 90°. $\vec{r}$ and $\vec{x}_n$ respectively represent the location vectors of the receiver and the n^{th} array element relative to the array phase centre. '$[\cdot]^T$' denotes vector transpose operator.

For isotropic antenna patterns, i.e., $\boldsymbol{AP}_n(\theta) = 1$ ($n = 1, 2, \ldots, N$), and uniform array element spacing ($|\vec{x}_{n+1} - \vec{x}_n|$) of one half wavelength, the electric far field component $\boldsymbol{E}$ is solely determined by element excitations ($\boldsymbol{A}_n$), (2),

$$\boldsymbol{E}(\theta) = \sum_{n=1}^{N} \left(\boldsymbol{A}_n \cdot e^{j\pi\left(n - \frac{N+1}{2}\right)\cos\theta} \right) \tag{2}$$

The term $e^{-j\vec{k}\vec{r}} / |\vec{r}|$ is dropped, since it is a constant complex scaling factor for the electric field $\boldsymbol{E}$ in all directions.

Generally, in a conventional transmitter, here we assume all the antenna elements are actively excited, see Fig. 2, prior to radiation by the antenna array elements, information data is modulated digitally at baseband, up-converted, and then identically distributed to each antenna element via a beam-forming network. Since the beam-forming network is linear and usually is

made adaptive at the channel fading rate, its complex gain $\boldsymbol{G}_n$ for each n can be regarded as a constant with respect to the modulation rate which is generally much faster than the channel fading rate. Thus far-field electric field $\boldsymbol{E}_m$ is a scaled version (with a complex weights $\boldsymbol{M}$) of modulated data $\boldsymbol{D}_m$ at each direction, (3), where subscript 'm' refers to the m^{th} symbol transmitted. As a consequence the modulation format, namely the constellation patterns in IQ space, is preserved in all spatial directions. Operator '$(\cdot)^*$' denotes complex conjugation.

$$\boldsymbol{E_m}(\theta)=\sum_{n=1}^{N}\left(\underbrace{\boldsymbol{D_m}\cdot\boldsymbol{G_n^*}}_{\boldsymbol{A_{mn}}}\cdot e^{j\pi\left(n-\frac{N+1}{2}\right)\cos\theta}\right)=\boldsymbol{D_m}\cdot\underbrace{\sum_{n=1}^{N}\left(\boldsymbol{G_n^*}\cdot e^{j\pi\left(n-\frac{N+1}{2}\right)\cos\theta}\right)}_{\boldsymbol{M}} \tag{3}$$

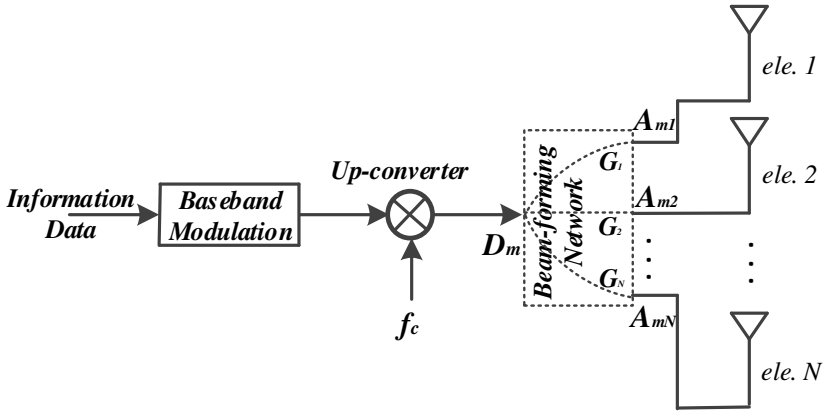

Fig. 2. Conventional 'non-DM' transmitter array architecture [10].

For DM systems, in order to achieve direction-dependent signal formats transmission, another degree of freedom has to be introduced. This is achieved by varying $\boldsymbol{G}_n$, and hence $\boldsymbol{M}$ in (3), at the modulation rate during data transmission in order to release the direct dependence of $\boldsymbol{E}_m$ on $\boldsymbol{D}_m$, in other words to distort constellation patterns along unsecured spatial directions. The updated $\boldsymbol{G}_n$ and $\boldsymbol{M}$ are denoted as $\boldsymbol{G}_{mn}$ and $\boldsymbol{M}_m$ respectively. In a DM transmitter, $\boldsymbol{G}_{mn}$ is updated at the modulation rate as is $\boldsymbol{D}_m$.

$$\boldsymbol{E_m}(\theta)=1\cdot\sum_{n=1}^{N}\left(\left(\boldsymbol{D}_m\boldsymbol{G}_{mn}^*\right)\cdot e^{j\pi\left(n-\frac{N+1}{2}\right)\cos\theta}\right) \tag{4}$$

$$\boldsymbol{E_m}(\theta)=\begin{bmatrix}\boldsymbol{D}_m\boldsymbol{G}_{m1}^*\\ \boldsymbol{D}_m\boldsymbol{G}_{m2}^*\\ \text{M}\\ \boldsymbol{D}_m\boldsymbol{G}_{mN}^*\end{bmatrix}\cdot\begin{bmatrix}1\cdot e^{j\pi\left(1-\frac{N+1}{2}\right)\cos\theta}\\ 1\cdot e^{j\pi\left(2-\frac{N+1}{2}\right)\cos\theta}\\ \text{M}\\ 1\cdot e^{j\pi\left(N-\frac{N+1}{2}\right)\cos\theta}\end{bmatrix} \tag{5}$$

By re-writing (3) as (4) and (5) for DM case, two interpretations can be drawn. The first, from a microwave engineering perspective, (4), $\left(\boldsymbol{D_m}\cdot\boldsymbol{G}_{mn}^*\right)^*$ can be considered as the complex gain,

$\boldsymbol{G}'_{mn}$, of a baseband information data controlled beam-forming network, into which an RF carrier f_c, instead of the modulated data stream $\boldsymbol{D}_m$, is injected, Fig. 3. This analogue DM architecture in Fig. 3 is actually the DM structures developed or used in [13, 18, 19, 23–26, 28, 30–32]. Alternatively, from a signal processing aspect, (5), $\boldsymbol{D}_m \cdot \boldsymbol{G}^*_{mn}$ can be regarded as uniquely weighted m^{th} data fed into the n^{th} array element. This weighting is readily implemented at baseband prior to up-conversion if the digital DM architecture presented here as Fig. 4 were to be used.

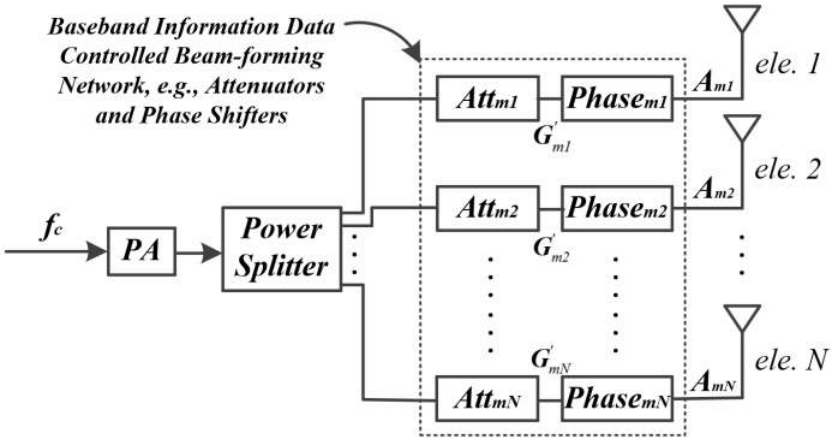

Fig. 3. Generic analogue active DM transmitter architecture [10].

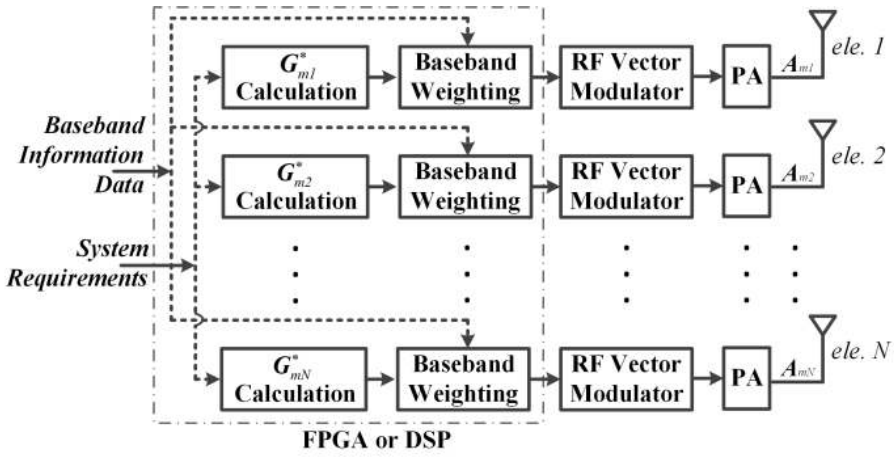

Fig. 4. Generic digital DM transmitter architecture [10].

2.2 Vector Representations for DM Arrays

Since there are several different ways to implement a DM system as discussed in Section 2.1, we require a description technique which is architecture independent and which lends itself to both analysis and synthesis of any class of DM structures. In this section we analyse the requirements that array excitations $\boldsymbol{A}_{mn}$ need to satisfy for a DM transmitter, regardless of the means of generating $\boldsymbol{A}_{mn}$.

The two key properties of a DM transmitter which we wish to establish are:

- Preservation of the transmitted signal format (standard constellation pattern in IQ space) along a pre-specified secure communication direction θ_0;
- Distortion of constellation patterns along all other unsecured communication directions.

From a signal processing perspective, $\boldsymbol{E}$ in (2) can be regarded as a detected constellation point in IQ space at receiver sides, denoted as $\boldsymbol{C}_m$ for the m^{th} symbol transmitted, (6),

$$\boldsymbol{C}_m(\theta) = \sum_{n=1}^{N} \underbrace{\left(\boldsymbol{A}_{mn} \cdot e^{j\pi\left(n-\frac{N+1}{2}\right)\cos\theta} \right)}_{\boldsymbol{B}_{mn}(\theta)} \tag{6}$$

For each symbol transmitted, the vector summation of $\boldsymbol{B}_{mn}$ has to yield the standard constellation point $\boldsymbol{C}_{m\_st}$ in IQ space along, and only along, the direction θ_0, which, in mathematical description, is expressed in (7).

$$\sum_{n=1}^{N} \boldsymbol{B}_{mn}(\theta_0) = \boldsymbol{C}_{m\_st}(\theta_0) \tag{7}$$

From (6), by scanning the observation angle θ, the constellation track in IQ space, $\boldsymbol{C}_m(\theta)$, of the m^{th} symbol can be obtained. General properties of constellation tracks can be observed from (6), and are summarized as below,

a) For an array with odd number elements, constellation tracks are closed loci, in some extreme cases, these loci collapse to line segments, starting point (θ = 0º) always overlaps with end point (θ = 180º). For the case of even number elements, $\boldsymbol{C}_m(0º) = -\boldsymbol{C}_m(180º)$. When the array element spacing is changed, the start and end angle will change accordingly;

b) Changing the desired communication direction θ_0 does not affect the shape of the constellation track pattern, it determines only where the tracks start (θ = 0º) and end (θ = 180º);

c) Different vector paths (trajectories of the vector summation, $\sum_{n=1}^{N} \boldsymbol{B}_{mn}(\theta_0)$) inevitably lead to different constellation tracks. This is guaranteed by the orthogonality property of $e^{jn\pi\cos\theta}$ for different n within the spatial range 0º to 180º;

d) For the q^{th} symbol transmitted, if $\boldsymbol{B}_{qn}(\theta_0)$ are the scaled $\boldsymbol{B}_{mn}(\theta_0)$ with the same scaling factor $\boldsymbol{K}$ for each n, the constellation track $\boldsymbol{C}_q(\theta)$ is also the scaled $\boldsymbol{C}_m(\theta)$ with the scaling factor $\boldsymbol{K}$.

Properties (c) and (d) mean that constellation distortion at other directions can be guaranteed if vectors $[\boldsymbol{B}_{q1}(\theta_0)\ \boldsymbol{B}_{q2}(\theta_0)\ \bullet\bullet\bullet\ \boldsymbol{B}_{qN}(\theta_0)]$ and $[\boldsymbol{B}_{m1}(\theta_0)\ \boldsymbol{B}_{m2}(\theta_0)\ \bullet\bullet\bullet\ \boldsymbol{B}_{mN}(\theta_0)]$ are linearly independent, see (8). Here the q^{th} and the m^{th} symbols in the data stream are different modulated symbols.

$$\left[\boldsymbol{B}_{q1}(\theta_0)\quad \boldsymbol{B}_{q2}(\theta_0)\quad \text{L}\quad \boldsymbol{B}_{qN}(\theta_0)\right] \neq \boldsymbol{K}\cdot\left[\boldsymbol{B}_{m1}(\theta_0)\quad \boldsymbol{B}_{m2}(\theta_0)\quad \text{L}\quad \boldsymbol{B}_{mN}(\theta_0)\right] \tag{8}$$

The combination of (7) and (8) forms the necessary conditions for DM transmitter arrays. Thus the requirement for the DM array excitations $\boldsymbol{A}_{mn}$ can then be obtained by (6).

With the DM vector model described above the static and dynamic DM transmitters are defined below. This classification facilitates the discussions of DM assessment metrics and DM synthesis approaches that will be presented in Sections III and IV respectively.

Definition: If along the DM secure communication direction the vector path in IQ space reaching each unique constellation point is independent and fixed, which results in a distorted, but static with respect to time, constellation pattern along other spatial directions, the transmitters are termed 'static DM'; on the contrary if the vector paths were randomly re-selected, on a per transmitted symbol basis in order to achieve the same constellation symbol in the desired direction, then the symbol transmitted at the different time slots in the data stream along spatial directions other than the prescribed direction would be scrambled dynamically and randomly. This we call the 'dynamic DM' strategy.

With the definition above most of the DM transmitters reported in the open literature, e.g., [13, 14, 18–33], fall into the static DM category, while the DM systems reported in [17, 34–37], involving time as another viable to update system settings, can be labelled as dynamic.

III. Metrics for Assessing Performance of DM Systems

To gain better cohesion with regard to DM system assessment comparability this section summarises all the available DM performance metrics.

In some previous DM work, e.g., [22, 30–32], the authors described DM properties that were obtained by certain physical arrangements or synthesis methods; however no performance assessments were made. In [18–21, 23–25] normalized error rate was adopted, but no magnitude and phase reference of detected constellation patterns were defined. Furthermore since channel noise and coding strategy was not considered, this metric is not able to capture differences in performance if (a) a constellation symbol is constrained within its optimal compartment for decoding, e.g., one quadrant for QPSK, but locates at different positions within that compartment; (b) a constellation symbol is out of its compartment but falls into a different compartment. These omissions make the 'error rate' of a DM system difficult to use for systematic assessment. In [17] an error-vector-magnitude-like (EVM-like) figure of merit, $\mathrm{FOM_{DM}}$, for describing the capability of constellation pattern distortion in a DM system was defined. However, it suffers the same problem of no channel noise and coding strategy consideration. It is also found that its computation can yield different values for static and dynamic DM systems due to different reference constellation patterns. In [33] bit error rate (BER) was used to assess the performance of a QPSK DM system, but no information about how it is calculated was provided. While in [26–29] a closed-form QPSK BER lower bound equation for static DM system evaluation was proposed, which was corrected and further extended in [13].

In [12] the metrics for assessing the performance of DM systems were formally discussed. It was shown that for static DM systems BER, calculated from either closed-form equations or

transmitting random data streams, and secrecy rate [38], normally used in information theory community, were applicable for system performance evaluation, whereas EVM-like metrics, although the channel noise and coding strategy were considered, did not perform well. For dynamic DM systems under the scenarios of zero-mean Gaussian distributed orthogonal interference, EVM-like metrics, BER, and secrecy rate were equivalent and can be converted into each other. For other interference distributions no closed-form BER and secrecy rate equations were available. Here the concept of orthogonal interference or vector can be found in [11] and will also be presented in Section 4.1.

In order to provide readers a clear picture on metrics for assessing performance of DM systems, all the findings presented in [12] are summarized in Table 1.

Table 1. Summaries of Metrics for DM System Performance Assessment

			Dynamic DM			
		Static DM	Zero-mean Gaussian orthogonal vectors	Zero-mean Non-Gaussian orthogonal vectors	Non-zero-mean orthogonal vectors	Calculation complexity
EVM_{DM}		–	+	–	–	Low
BER	Closed-form equation	•	•	–	–	Low
	Data stream simulation	+	+	+	+	Medium
Secrecy rate	Numerical calculus [39, 40]	+	+	–	–	Medium
	Bit-wise [41]	–	+	–	–	High

'+': Metric works
'•': Metric works for QPSK, but not for higher order modulations
'–': Metric cannot be calculated or does not work

IV. Synthesis Approaches for DM Transmitter Arrays

Prior to the recent efforts in [11, 14–16], the previous DM synthesis attempts were closely bounded up with the physical DM transmitter structures. For passive DM transmitter arrays [20–22], termed by authors near-field direct antenna modulation (NFDAM), which rely on the complex transformation between near-field electromagnetic boundaries and far-field behaviours, there is no analytical means to map transmitter settings to vector paths in IQ space, and ultimately to the constellation tracks and secrecy performance. As a consequence, it seems nearly impossible for a mathematically rigorous passive DM transmitter, satisfying the (7) and (8) in Section II, to be synthesized. Thus it is natural that no effective synthesis methods other than trial and error can be effected, although the search area can be shrunk using optimization as in [42].

On the contrary, in terms of the active DM arrays [26–29], due to the independent excitation of each array element, we can readily transform array excitations and array physical arrangements into vector paths in IQ space in an analytical fashion. Thus a fit-for-purpose cost function can be established for DM system optimization. Normally the cost functions link the BER spatial

distributions to the array settings. By minimizing the values of the cost functions through population-based optimization algorithms, DM transmitter arrays can be synthesized. However, it should be noted that the decoding functionality of the receiver has a major influence on the quality of recovered data and should be well defined during the BER-driven synthesis [13].

While investigating the DM architectures in [34–37], it was realized that, unlike the DM systems described in [20–22, 26–29], under their prescribed working mechanisms no synthesis is required, since in these systems the DM requirements of the (7) and (8) are automatically satisfied. This, with the help of the orthogonal vector concept [11], indicates that injected interference constantly stays orthogonal to conjugated channel vectors along the intended communication directions. Similarly the Fourier lens enabled DM transmitters, which were recently proposed in [17], fall into the same category.

In order to generalize the DM synthesis approaches, based on the actively excited 1-D transmitter arrays, we should focus on seeking appropriate array excitations, which enable DM characteristics and improve secrecy performance, irrespective of the means of generating those excitations. With the obtained excitations, the DM transmitters can be constructed by using either analogue, e.g., see Fig. 3, or digital means, e.g., see Fig. 4, or alternatively employing suitably featured beam-forming networks.

In Section 4.1 a smart concept, i.e., orthogonal vector, is introduced, and is utilized for DM transmitter array synthesis [11]. This approach is compatible for both static and dynamic DM transmitters. In order to meet some other DM system requirements, e.g., detected BER spatial distributions [13], far-field radiation patterns [14, 15], and orthogonal interference distributions [16], three more synthesis approaches are briefly described in Sections 4.2. These approaches can be regarded as seeking a subset of orthogonal vectors under certain system constraints.

4.1 Orthogonal Vector Approach for DM Array Synthesis

In Section 2.2 it is showed that when the same constellation symbol detected along the desired communication direction is reached via different vector paths in IQ space, the resulting constellation tracks are altered accordingly. This leads to the constellation pattern distortion along spatial directions other than the prescribed direction, which is the key property of DM systems. In other words, it is the difference vector between each two vector paths selected to achieve a same standard constellation point in IQ space that enables the DM characteristics. This difference vector is defined as the orthogonal vector, since it is always orthogonal to the conjugated channel vector along the intended spatial direction.

A 1-D 5-element array with half wavelength spacing is taken as an example below to explain the orthogonal vector concept. It is assumed that each antenna element has an identical isotropic far-field radiation pattern.

The channel vector for this system along the desired communication direction θ_0 in free space is

$$\underset{\mathbf{H}}{\mathbf{V}}(\theta_0)=\left[\underbrace{e^{j2\pi\cos\theta_0}}_{\boldsymbol{H}_1}\quad\underbrace{e^{j\pi\cos\theta_0}}_{\boldsymbol{H}_2}\quad\underbrace{e^{j0}}_{\boldsymbol{H}_3}\quad\underbrace{e^{-j\pi\cos\theta_0}}_{\boldsymbol{H}_4}\quad\underbrace{e^{-j2\pi\cos\theta_0}}_{\boldsymbol{H}_5}\right]^T \tag{9}$$

If the excitation signal vectors at the array input, $[\boldsymbol{A}_{m1}\ \boldsymbol{A}_{m2}\ \ldots\ \boldsymbol{A}_{m5}]^T$, for the same symbol transmitted at the u^{th} and v^{th} time slots are chosen to be

$$\underset{\mathbf{S}}{\mathbf{V}}_u=\left[\underbrace{e^{j\left(-\frac{\pi}{4}+2\pi\cos\theta_0\right)}}_{\boldsymbol{S}_{u1}}\quad\underbrace{e^{j\left(\frac{\pi}{4}+\pi\cos\theta_0\right)}}_{\boldsymbol{S}_{u2}}\quad\underbrace{e^{j\left(\frac{\pi}{4}\right)}}_{\boldsymbol{S}_{u3}}\quad\underbrace{e^{j\left(\frac{\pi}{4}-\pi\cos\theta_0\right)}}_{\boldsymbol{S}_{u4}}\quad\underbrace{e^{j\left(\frac{3\pi}{4}-2\pi\cos\theta_0\right)}}_{\boldsymbol{S}_{u5}}\right]^T \tag{10}$$

and

$$\underset{\mathbf{S}}{\mathbf{V}}_v=\left[\underbrace{e^{j\left(\frac{\pi}{4}+2\pi\cos\theta_0\right)}}_{\boldsymbol{S}_{v1}}\quad\underbrace{e^{j\left(\frac{\pi}{4}+\pi\cos\theta_0\right)}}_{\boldsymbol{S}_{v2}}\quad\underbrace{e^{j\left(-\frac{\pi}{4}\right)}}_{\boldsymbol{S}_{v3}}\quad\underbrace{e^{j\left(\frac{3\pi}{4}-\pi\cos\theta_0\right)}}_{\boldsymbol{S}_{v4}}\quad\underbrace{e^{j\left(\frac{\pi}{4}-2\pi\cos\theta_0\right)}}_{\boldsymbol{S}_{v5}}\right]^T \tag{11}$$

The received vector paths in IQ space along this spatial direction θ_0 are

$$\begin{aligned}\underset{\mathbf{B}}{\mathbf{V}}_u&=\underset{\mathbf{H}}{\mathbf{V}}^*(\theta_0)\circ\underset{\mathbf{S}}{\mathbf{V}}_u=\left[\underbrace{\boldsymbol{H}_1^*\cdot\boldsymbol{S}_{u1}}_{\boldsymbol{B}_{u1}}\quad\underbrace{\boldsymbol{H}_2^*\cdot\boldsymbol{S}_{u2}}_{\boldsymbol{B}_{u2}}\quad\underbrace{\boldsymbol{H}_3^*\cdot\boldsymbol{S}_{u3}}_{\boldsymbol{B}_{u3}}\quad\underbrace{\boldsymbol{H}_4^*\cdot\boldsymbol{S}_{u4}}_{\boldsymbol{B}_{u4}}\quad\underbrace{\boldsymbol{H}_5^*\cdot\boldsymbol{S}_{u5}}_{\boldsymbol{B}_{u5}}\right]^T\\&=\left[e^{-j\frac{\pi}{4}}\quad e^{j\frac{\pi}{4}}\quad e^{j\frac{\pi}{4}}\quad e^{j\frac{\pi}{4}}\quad e^{j\frac{3\pi}{4}}\right]^T\end{aligned} \tag{12}$$

and

$$\begin{aligned}\underset{\mathbf{B}}{\mathbf{V}}_v&=\underset{\mathbf{H}}{\mathbf{V}}^*(\theta_0)\circ\underset{\mathbf{S}}{\mathbf{V}}_v=\left[\underbrace{\boldsymbol{H}_1^*\cdot\boldsymbol{S}_{v1}}_{\boldsymbol{B}_{v1}}\quad\underbrace{\boldsymbol{H}_2^*\cdot\boldsymbol{S}_{v2}}_{\boldsymbol{B}_{v2}}\quad\underbrace{\boldsymbol{H}_3^*\cdot\boldsymbol{S}_{v3}}_{\boldsymbol{B}_{v3}}\quad\underbrace{\boldsymbol{H}_4^*\cdot\boldsymbol{S}_{v4}}_{\boldsymbol{B}_{v4}}\quad\underbrace{\boldsymbol{H}_5^*\cdot\boldsymbol{S}_{v5}}_{\boldsymbol{B}_{v5}}\right]^T\\&=\left[e^{j\frac{\pi}{4}}\quad e^{j\frac{\pi}{4}}\quad e^{-j\frac{\pi}{4}}\quad e^{j\frac{3\pi}{4}}\quad e^{j\frac{\pi}{4}}\right]^T\end{aligned} \tag{13}$$

These are shown in Fig. 5 (a) and (b), respectively. Operator '$\circ$' denotes Hadamard product of two vectors.

The vector summations in $\boldsymbol{B}_{un}$, and $\boldsymbol{B}_{vn}$ (n = 1, 2, 3, 4, 5) can be calculated as $\underset{\mathbf{H}}{\mathbf{V}}^{\dagger}(\theta_0)\underset{\mathbf{S}}{\mathbf{V}}_u$ and $\underset{\mathbf{H}}{\mathbf{V}}^{\dagger}(\theta_0)\underset{\mathbf{S}}{\mathbf{V}}_v$, both reaching position $3\cdot e^{j\pi/4}$ in IQ space. '$(\cdot)^{\dagger}$' denotes complex conjugate transpose (Hermitian) operator.

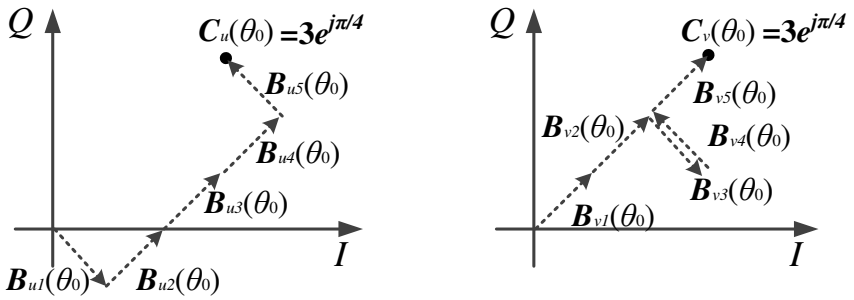

(a) (b)

Fig. 5. Illustration example of two vector paths derived from two different excitation settings.

The difference between these two excitation signal vectors is

$$\Delta\mathbf{S} = \mathbf{S}_v - \mathbf{S}_u = \sqrt{2}\left[e^{j\left(\frac{\pi}{2}+2\pi\cos\theta_0\right)} \quad 0 \quad e^{-j\frac{\pi}{2}} \quad e^{j\pi(1-\cos\theta_0)} \quad e^{-j2\pi\cos\theta_0} \right]^T \tag{14}$$

which is orthogonal to the conjugated channel vector $\mathbf{H}^*(\theta_0)$ since $\mathbf{H}^*(\theta_0)\cdot\Delta\mathbf{S} = 0$. This $\Delta\mathbf{S}$ is the orthogonal vector defined in this section.

With the help of the orthogonal vector concept, a generalized DM synthesis approach was developed in [11]. The synthesized DM transmitter array excitation vector $\mathbf{S}_{ov}$ takes the form

$$\mathbf{S}_{ov} = \mathbf{\Lambda} + \mathbf{W}_{ov} \tag{15}$$

$\mathbf{\Lambda}$ is a vector with each entry of array excitations before injecting the orthogonal vector $\mathbf{W}_{ov}$, which is orthogonal to the conjugated channel vector, $\mathbf{H}_{ov}^*$. Denote $\mathbf{Q}_p$ (p = 1, 2, …, N−1) to be the orthonormal basis in the null space of $\mathbf{H}^*$, then $\mathbf{W}_{ov} = \frac{1}{N-1}\cdot\sum_{p=1}^{N-1}\left(\mathbf{Q}_p \cdot v_p\right)$. Here $\mathbf{\Lambda}$ is defined as excitations of non-DM beam steering arrays. This excitation contains the information symbol $\boldsymbol{X}$ to be transmitted, e.g., $e^{j\pi/4}$ corresponds to the QPSK symbol '11'.

Take a transmitter array consisting of 1-D 5-element half-wavelength spaced antenna elements with isotropic radiation patterns, modulated for QPSK for 45º secure communication as an example, Fig. 6 shows simulated far-field patterns in the synthesized dynamic DM system for 100 random QPSK symbols transmitted when the v_p are circularly symmetric independent and identically distributed (i.i.d.) complex Gaussian distributed variables with variance σ_v^2 of 0.8. From a receivers' point of view, the far-field radiation patterns can be interpreted as detected constellation patterns in IQ space along each direction. Thus it can be concluded that a standard QPSK constellation pattern, i.e., uniform magnitudes and 90º separated phases, are preserved only along the selected secure communication direction, 45º in this example.

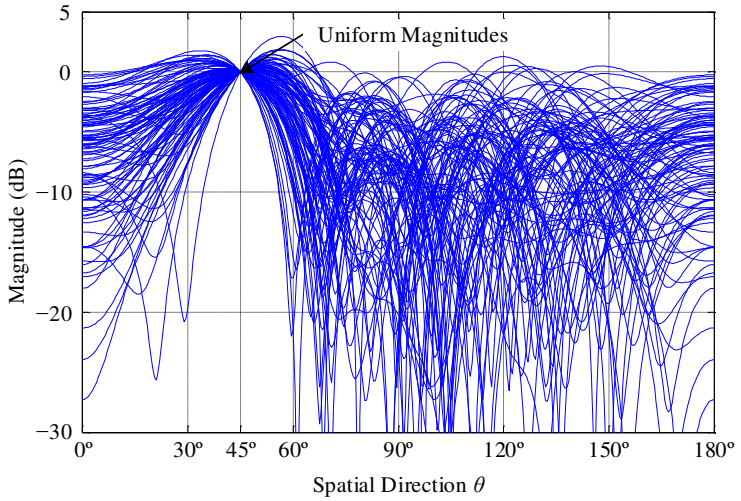

(a)

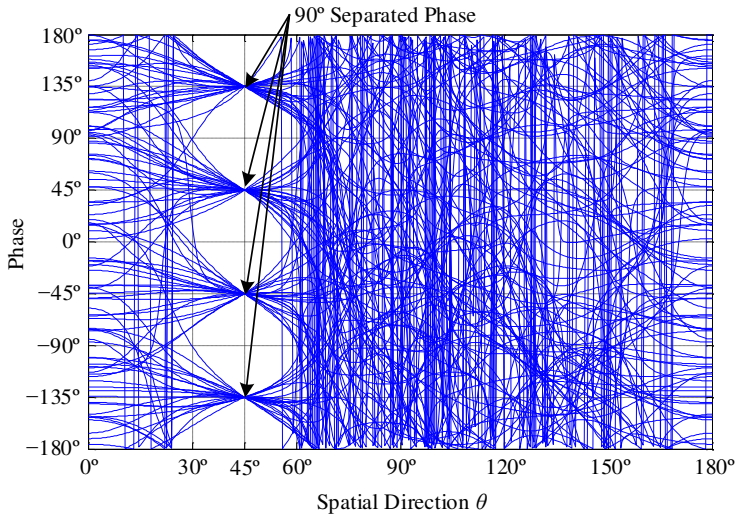

(b)

Fig. 6. Simulated far-field (a) magnitude and (b) phase patterns of the 5-element dynamic QPSK DM transmitter array for 100 random QPSK symbols with circularly symmetric i.i.d. complex Gaussian distributed v_p ($\sigma_v^2 = 0.8$).

During the synthesis of DM arrays from the non-DM beam steering arrays two parameters which are crucial to system performance, need to be discussed. One is the length of each excitation vector. From a practical implementation perspective the square of the excitation vector should fall into the linear range of each power amplifier (PA) located within each RF path. The other is the extra power injected into the "non-DM" array. To describe this extra power the DM power efficiency ($\mathrm{PE_{DM}}$) is defined,

$$\mathrm{PE_{DM}} = \frac{\sum_{i=1}^{I}\left(\sum_{n=1}^{N}\left|\boldsymbol{\Lambda}_{in}\right|^2\right)}{\sum_{i=1}^{I}\left(\sum_{n=1}^{N}\left|\boldsymbol{S}_{ov\_in}\right|^2\right)}\times 100\% = \frac{\sum_{i=1}^{I}\left(\sum_{n=1}^{N}\left|\boldsymbol{B}_{in\_nonDM}\right|^2\right)}{\sum_{i=1}^{I}\left(\sum_{n=1}^{N}\left|\boldsymbol{B}_{in\_DM}\right|^2\right)}\times 100\% \tag{16}$$

where I is, for static DM, the number of modulation states, e.g., 4 for QPSK, or, for dynamic DM, the symbol number T in a data stream. $\boldsymbol{\Lambda}_{in}$ and $\boldsymbol{S}_{ov\_in}$ are the n^{th} array element excitation

for the i^{th} symbol in the non-DM array and in the synthesized DM array respectively. In noiseless free space their modulus equal to the normalized modulus of corresponding $\boldsymbol{B}_{in\_nonDM}$ and $\boldsymbol{B}_{in\_DM}$ from the receiver side perspective. Generally the larger the allowable range of the excitation vector lengths are, and the lower $\mathrm{PE_{DM}}$ is, the better the DM system secrecy performance that can be achieved, see the simulated BER examples in Fig. 7. In other words, the enhanced secrecy performance, i.e., narrower main BER beams and more suppressed BER sidelobes are achieved at the cost of more energy radiated into the space by the DM arrays.

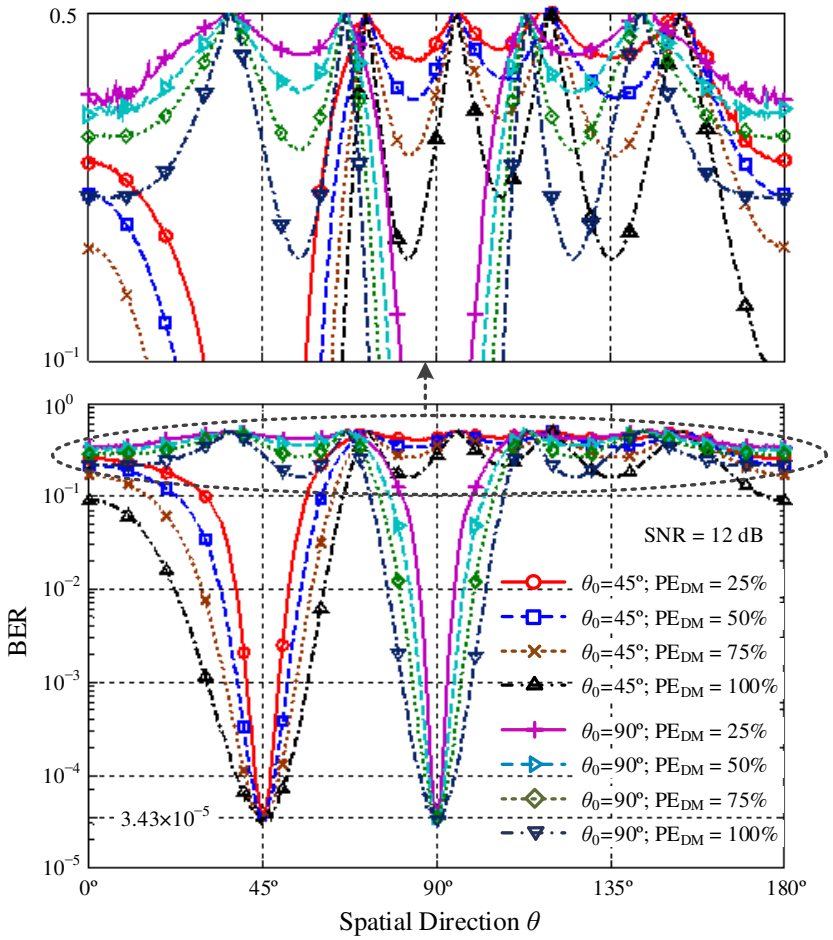

Fig. 7. Simulated BER spatial distributions in dynamic QPSK DM systems with different $\mathrm{PE_{DM}}$s for 45° and 90° secure communications. Signal to noise ratio (SNR) is set to 12 dB.

The $\mathrm{PE_{DM}}$s in this example are determined by the parameter v_p that is used for controlling the power of the generated orthogonal vectors $\boldsymbol{W}_{ov}$, (17) and (18).

$$\mathrm{PE}_{\mathrm{DM}\_i} = \frac{1}{1+\sum_{p=1}^{N-1}\left(\frac{1}{N-1}\cdot v_p\right)^2}\times 100\% \tag{17}$$

$$\mathrm{PE}_{\mathrm{DM}} = \frac{1}{I}\cdot\sum_{i=1}^{I}\mathrm{PE}_{\mathrm{DM}\_i} \tag{18}$$

It needs to be pointed out that for the example in Fig. 7 v_p is not set to be a Gaussian distributed

viable, instead we constrain $\sum_{p=1}^{N-1}\left(\frac{1}{N-1}\cdot v_p\right)^2$ to be a constant according to the required PE_{DM}. This avoids very large array excitations from being synthesized as they are impractical in physical realizations.

4.2 DM Array Synthesis Approaches When Imposing Some Extra System Requirements

In Section 4.1 the universal DM synthesis method, i.e., the orthogonal vector approach, is presented. However, in some application scenarios, some other requirements on DM system properties may need to be considered. These requirements, or constraints, which have been investigated, include the BER spatial distribution, the array far-field radiation characteristics, and the interference spatial distribution. All three synthesis methods associated with each scenario can be viewed as seeking a subset of orthogonal vectors that satisfy prescribed DM system requirements.

The BER-driven [13] and the constrained array far-field radiation pattern [14, 15] DM synthesis approaches share a similar idea, i.e., via the iterative transformations between the array excitations and the required DM properties, namely the BER spatial distributions and the array far-field radiation patterns, the constraints on DM characteristics can be imposed. Since iteration processes are involved, these two methods are not suitable for dynamic DM synthesis.

Another DM array far-field pattern separation synthesis approach was developed in [16]. Here by virtue of the far-field null steering approach, the DM array far-field radiation patterns can be separated into information patterns, which describe information energy projected along each spatial direction, and interference patterns, which represent disturbance on genuine information. By this separation methodology we can identify the spatial distribution of information transmission and hence focus interference energy into the most vulnerable directions with regard to interception, i.e., information sidelobes, and in doing so submerge leaked information along unwanted directions. This method is closely linked to the orthogonal vector approach. In fact the separated interference patterns can be considered as far-field patterns generated by the injected orthogonal vectors. However, it is more convenient to apply constraints, such as interference spatial distribution, with the pattern separation approach. This approach is compatible with both static and dynamic DM systems.

The relationships among the four DM synthesis approaches are illustrated in Fig. 8.

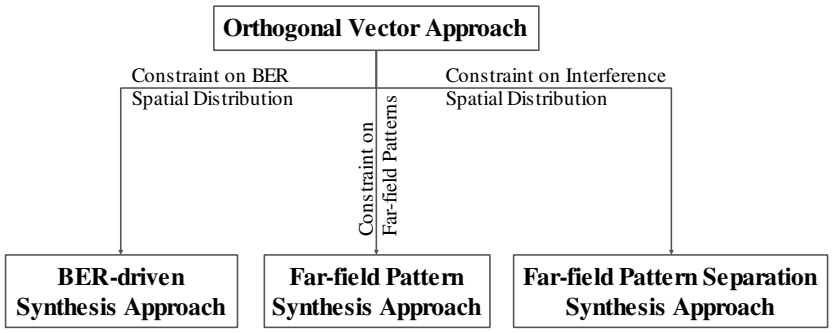

Fig. 8. Relationships among the four DM synthesis approaches.

V. DM demonstrators

Up to date there have been four DM demonstrators built for real-time data transmission.

The first demonstrator was constructed based on the passive DM architecture in 2008 [20]. Since there are no effective synthesis methods associated with this type of DM structure, as was discussed in Section IV, no further development in this branch has been made afterwards.

Instead of passively excited DM array elements, the actively excited DM array demonstrator was built based on the analogue structure in Fig. 2 [28]. Since the iterative BER-driven synthesis approach was adopted, only the static DM transmitter was achieved.

A 7-element digital DM demonstrator for 2.4 GHz operation [43] was realised with the help of the Wireless Open-Access Research Platform (WARP) [44]. The block diagram and the photograph of the experimental setup are illustrated in Figs. 9 and 10 respectively. This digital DM architecture is compatible with any synthesis methods presented in Sections 4.1 and 4.2.

The other DM demonstrator [45] can be considered as hardware realizations of the orthogonal vector DM synthesis approach. This promising arrangement in [45] utilised the beam orthogonality property possessed by Fourier beam-forming networks to orthogonally inject information and interference along the desired secure communication direction. This structure avoids the use of RF switches [20–22, 34–37] or analogue reconfigurable RF devices as in [18, 19, 23–32], thus leads to an effective step towards practical field applications. Several system level experiments based on a 13-by-13 Fourier Rotman lens for 10 GHz operation were conducted in an anechoic chamber. One is for general demonstration purpose, the video of which can be found in [46]. Another Fourier Rotman lens DM experiment employed the WARP boards, which allowed the digital modulation being adopted and BER being measured [45]. The experimental setup is illustrated in Figs. 11 and 12. The experimental results for both received constellation patterns and BER spatial distributions can be found in [45].

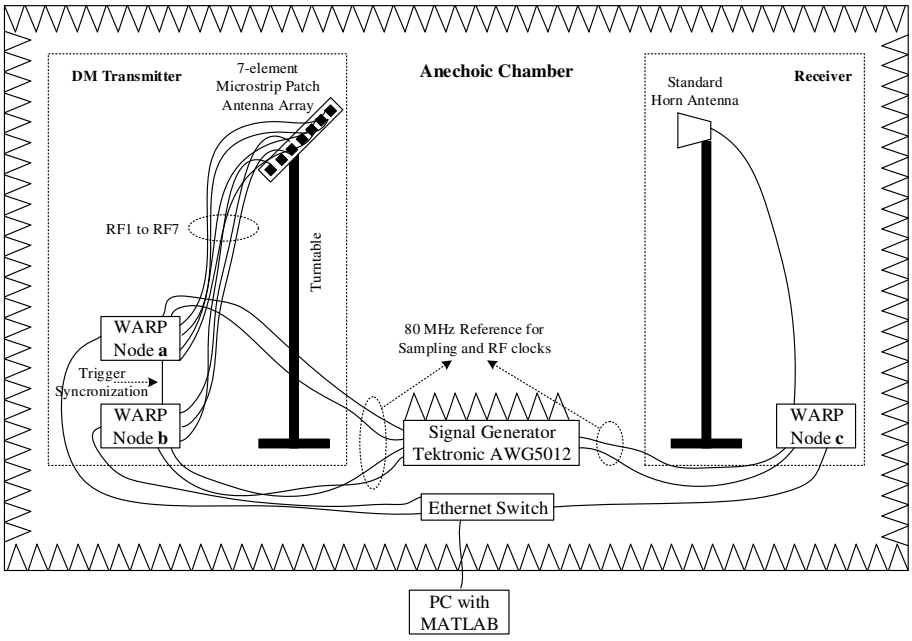

Fig. 9. Block diagram of the digital DM experimental setup [43].

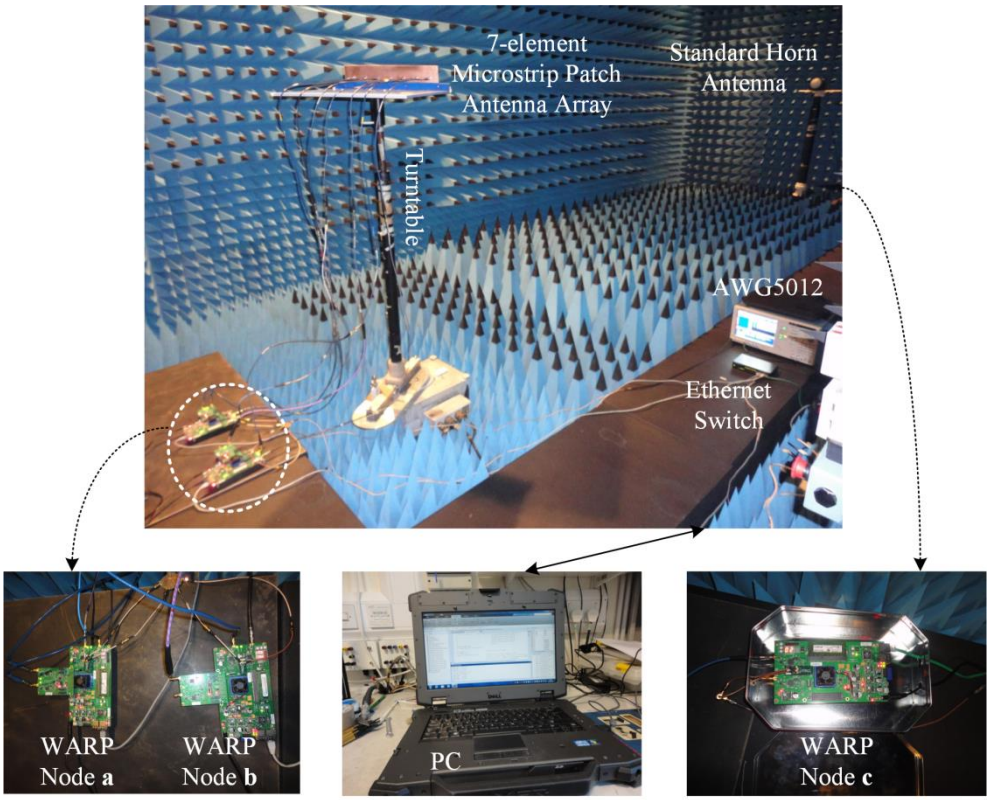

Fig. 10. Photographs of the digital DM experiment [43].

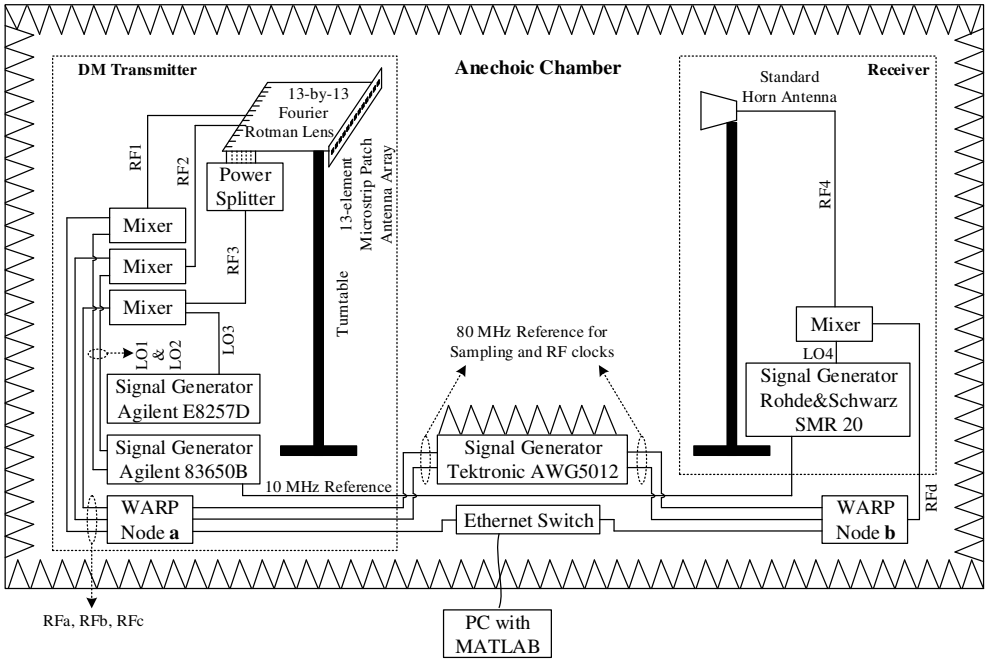

Fig. 11. Block diagram of the 13-by-13 Fourier Rotman lens DM experimental setup [45].

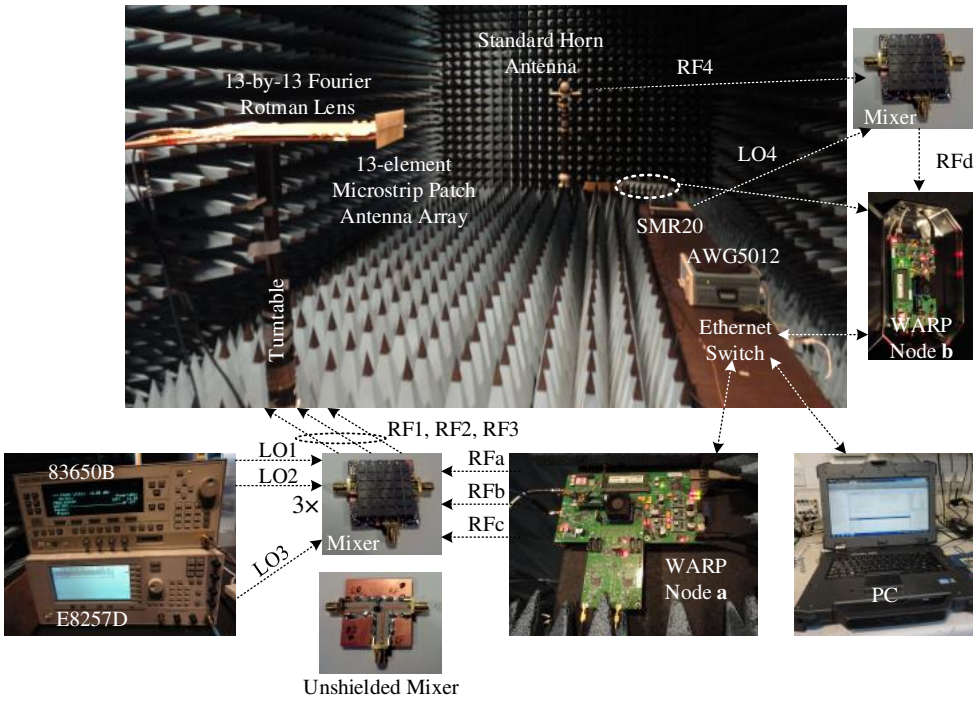

Fig. 12. Photographs of the 13-by-13 Fourier Rotman lens DM experiment [45].

The four DM demonstrators are summarized in Table 2.

Table 2. Summary of Four DM Demonstrators for Real-time Data Transmission

Article	[20]	[28]	[43]	[45]
DM architecture	Passive DM architecture	Analogue active DM architecture	Digital DM architecture	Fourier lens enabled DM architecture
Number of array elements	900	4	7	13
Synthesis method	trial and error	BER-driven	Orthogonal vector	Not required
Static or dynamic DM	Static	Static	Dynamic	Dynamic
Signal modulation	Non-standard	QPSK	DQPSK	DQPSK, DBPSK
Operating frequency	60 GHz	7 GHz	2.4 GHz	10 GHz
Bit rate	Unavailable	200 Kbps	5 Mbps	5 Mbps
Realization complexity	High	Medium	Medium	Low
Complexity of steering secure communication directions	High	High	Low	Low
Complexity of extension to other modulation types	High	Medium	Low	Low
Complexity of extension to multi-beam DM	High	High	Medium	Low

VI. Conclusions and recommendation for future work

This paper reviewed the DM technology in every aspect. Specifically Section II aimed to reveal the essence of DM technology and establish a universal DM description model. Section III was devoted to establishing universal figures of merit that allow direct comparison between different DM systems. The question of how a DM transmitter can be synthesized was addressed in Section IV, while the DM demonstrators for real-time data transmission, reported in the open literature were described and summarised in Section V.

From the conclusions above it can be seen that a holistic framework of DM technology has been attempted. Within this framework there are several important aspects that could be refined in the future, including;

- In [17] it was mentioned that it was the beam orthogonality property possessed by the FT-BFNs that enabled the DM functionality. However, in terms of successfully constructing DM transmitters it is required that only beam orthogonality along the desired communication direction occurs, i.e., the far-field patterns excited by the interference applied at the relevant beam ports have nulls along the direction where the main information beam projects. Whereas the main beam projected by the interference signal applied at each beam port lies at the null of the information pattern. Alignment of the nulls in this way is not strictly required as all that is needed for DM is that interference occurs everywhere except along the projected information direction. This means that the strict Fourier constraint can be relaxed to some extent. The extent of relaxation that can be applied could be investigated.

- It is imperative to extend DM technology for the applications under wireless multipath environment. Some initial attempts have been made in [30, 47] using simplified multipath models. To be more convincing a complex multipath channel model extracted from a real indoor environment would be helpful. Furthermore physical implementations and experiments on real-time data transmission are of works of interest.

- Almost all the reported DM work is on single-beam DM systems where only one information data stream is securely conveyed along one prescribed direction. It is natural to consider developing multi-beam DM systems, which have the capability of projecting multiple independent information data streams into different spatial directions, while simultaneously distorting information signal formats along all other unselected directions. This multi-beam DM concept was first suggested in 2008 [20]. However since then no real development has been made until the dual-beam Fourier lens based DM systems presented in [45]. Similar to single-beam DM, multi-beam DM technology should be systematically investigated from the aspects of the mathematical model, assessment metrics, synthesis approaches, and physical implementations.

ACKNOWLEDGEMENT

This work was sponsored by the Queen's University of Belfast High Frequency Research Scholarship.

REFERENCES

[1] Li, X.; Hwu J.; Ratazzi, E.P.: Using antenna array redundancy and channel diversity for secure wireless transmissions. Journal of Communications, Vol. 2, No. 3 (2007), 24-32.

[2] Mollin, R. A.: An introduction to cryptography. CRC Press, 2006

[3] William, S.: Cryptography and Network Security. 4th ed. Pearson Education India, 2006.

[4] Forouzan, B. A.: Cryptography and Network Security. McGraw-Hill, Inc., 2007.

[5] Bloch, M.; Barros, J.: Physical-Layer Security: From Information Theory to Security Engineering. Cambridge University Press, 2011.

[6] Wang, T.; Liu, Y.; Vasilakos, A.: Survey on channel reciprocity based key establishment techniques for wireless systems. Wireless Networks, Springer, 2015, available: http://dx.doi.org/10.1007/s11276-014-0841-8

[7] Chen, C.; Jensen, M. A.: Secret key establishment using temporally and spatially correlated wireless channel coefficients. Mobile Computing, IEEE Transactions on, Vol. 10 (2011), 205-215.

[8] Ahmadi, H.; Safavi-Naini, R.: Secret key establishment over a pair of independent broadcast channels. Information Theory and its Applications (ISITA), 2010 International Symposium on, 185-190, 2010.

[9] Mukherjee, A.; Fakoorian, S. A. A.; Huang, J.; Swindlehurst, A. L,: Principles of physical layer security in multiuser wireless networks: A survey. arXiv preprint arXiv:1011.3754, 2010.

[10] Ding, Y.; Fusco, V.: Vector representation of directional modulation transmitters. Antennas and Propagation (EuCAP), 2014 8th European Conference on, 332–336, 2014.

[11] Ding, Y.; Fusco, V.: A vector approach for the analysis and synthesis of directional modulation transmitters," Antennas and Propagation, IEEE Transactions on, Vol. 62 (2014), 361-370.

[12] Ding, Y.; Fusco, V.: Establishing metrics for assessing the performance of directional modulation systems," Antennas and Propagation, IEEE Transactions on, Vol. 62 (2014), 2745-2755.

[13] Ding, Y.; Fusco, V.: BER-driven synthesis for directional modulation secured wireless communication. International Journal of Microwave and Wireless Technologies, Vol. 6 (2014), 139-149.

[14] Ding, Y.; Fusco, V.: Directional modulation transmitter radiation pattern considerations. IET Microwaves, Antennas and Propagation, Vol. 7, No. 15 (2013), 1201-1206.

[15] Ding, Y.; Fusco, V.: Constraining directional modulation transmitter radiation patterns. IET Microwaves, Antennas and Propagation, Vol. 8, No. 15 (2014), 1408-1415.

[16] Ding, Y.; Fusco, V.: Directional modulation far-field pattern separation synthesis approach. IET Microwaves, Antennas and Propagation, Vol. 9, No. 1 (2015), 41-48.

[17] Zhang, Y.; Ding, Y.; Fusco, V.: Sidelobe modulation scrambling transmitter using Fourier Rotman lens. Antennas and Propagation, IEEE Transactions on, Vol. 61 (2013), 3900-3904.

[18] Shi, H.; Tennant, A.: Secure physical-layer communication based on directly modulated antenna arrays. Antennas and Propagation Conference (LAPC), 2012 Loughborough, 1-4, 2012.

[19] Shi, H.; Tennant, A.: Enhancing the security of communication via directly modulated antenna arrays. IET Microwaves, Antennas and Propagation, Vol. 7, No. 8 (2013), 606-611.

[20] Babakhani, A.; Rutledge, D. B.; Hajimiri, A,: Transmitter architectures based on near-field direct antenna modulation. Solid-State Circuits, IEEE Journal of, vol. 43 (2008), 2674-2692.

[21] Babakhani, A.; Rutledge, D.B.; Hajimiri, A.: Near-field direct antenna modulation. Microwave Magazine, IEEE, vol. 10 (2009), 36-46.

[22] Chang, A. H.; Babakhani, A.; Hajimiri, A.: Near-field direct antenna modulation (NFDAM) transmitter at 2.4GHz. Antennas and Propagation Society International Symposium, 2009 IEEE, 1-4, 2009.

[23] Shi, H.; Tennant, A.: Direction dependent antenna modulation using a two element array. Proc. 5th Eur. Conf. on Antennas and Propagation (EuCAP), 2011, 812-815, 2011.

[24] Shi, H.; Tennant, A.: Characteristics of a two element direction dependent antenna array. Antennas and Propagation Conference (LAPC), 2011 Loughborough, 1-4, 2011.

[25] Shi, H.; Tennant, A.: An experimental two element array configured for directional antenna modulation. Proc. 6th Eur. Conf. on Antennas and Propagation (EuCAP), 2012, 1624–1626, 2012.

[26] Daly, M. P.; Bernhard, J. T.: Directional modulation technique for phased arrays. Antennas and Propagation, IEEE Transactions on, vol. 57 (2009), 2633-2640.

[27] Daly, M. P.; Bernhard, J. T.: Beamsteering in pattern reconfigurable arrays using directional modulation. Antennas and Propagation, IEEE Transactions on, vol. 58 (2010), 2259-2265.

[28] Daly, M. P.; Daly, E. L.; Bernhard, J. T.: Demonstration of directional modulation using a phased array. Antennas and Propagation, IEEE Transactions on, vol. 58 (2010), 1545-1550.

[29] Daly, M. P.: 2012: Physical layer encryption using fixed and reconfigurable antennas. Ph.D. dissertation, Dept. Electrical and Computer Eng., University of Illinois at Urbana-Champaign.

[30] Shi, H.; Tennant, A.: Secure communications based on directly modulated antenna arrays combined with multi-path. Antennas and Propagation Conference (LAPC), 2013 Loughborough, 582-586, 2013.

[31] Shi, H.; Tennant, A.: Covert communication using a directly modulated array transmitter. Proc. 8th Eur. Conf. on Antennas and Propagation (EuCAP), 2014, 316–318, 2014.

[32] Shi, H.; Tennant, A.: Simultaneous, multi-channel, spatially directive data transmission using direct antenna modulation. Antennas and Propagation, IEEE Transactions on, Vol. 62, No. 1 (2014), 403–410.

[33] Hong, T.; Song, M.Z.; Liu, Y.: Dual-beam directional modulation technique for physical-layer secure communication. Antennas and Wireless Propagation Letters, IEEE, vol. 10 (2011), 1417-1420.

[34] Valliappan, N.; Lozano, A.; Heath, R. W.: Antenna subset modulation for secure millimeter-wave wireless communication. Communications, IEEE Transactions on, Vol. 61, No. 8 (2013), 3231-3245.

[35] Zhu, Q,; Yang, S.; Yao, R.; Nie, Z.: A directional modulation technique for secure communication based on 4D antenna arrays. Proc. 7th Eur. Conf. on Antennas and Propagation (EuCAP), 2013, 125-127.

[36] Zhu, Q,; Yang, S.; Yao, R.; Nie, Z.: Directional modulation based on 4-D antenna arrays. Antennas and Propagation, IEEE Transactions on, Vol. 62, No. 2 (2014), 621-628.

[37] Hong, T.; Song, M.Z.; Liu, Y.: RF directional modulation technique using a switched antenna array for physical layer secure communication applications. Progress In Electromagnetics Research, Vol. 116 (2011), 363-379.

[38] Csiszar, I.; Korner, J.: Broadcast channels with confidential messages. Information Theory, IEEE Transactions on, Vol. 24 (1978), 339-348.

[39] McIllree, P. E.: 1995: Channel capacity calculations for M-ary N-dimensional signal sets. M.E. thesis in Electronic Engineering, The University of South Australia.

[40] Stroud, A. H.: Approximate Calculation of Multiple Integrals. EnglewoodCliffs, New Jersey, Prentice-Hall, 1971, 23-52.

[41] Brink, S. T.: Convergence behavior of iteratively decoded parallel concatenated codes. Communications, IEEE Transactions on, Vol. 49, No. 10 (2001), 1727-1737.

[42] Lavaei, J.; Babakhani, A.; Hajimiri, A.; Doyle, J. C.: A study of near-field direct antenna modulation systems using convex optimization. American Control Conference (ACC), 2010, 1065-1072, 2010.

[43] Ding, Y.; Fusco, V.: Experiment of digital directional modulation transmitters. Forum for Electromagnetic Research Methods and Application Technologies (FERMAT), accepted for publication.

[44] WARP project. [Online]. Available: http://www.warpproject.org. [Accessed: 14-Jun-2014].

[45] Ding, Y.; Zhang, Y.; Fusco, V.: Fourier Rotman lens enabled directional modulation transmitter. International Journal of Antennas and Propagation, vol. 2015, Article ID 285986, 13 pages, 2015. doi:10.1155/2015/285986

[46] Fourier Rotman lens directional modulation demonstrator experiment. [Online]. Available: https://www.youtube.com/watch?v=FsmCcxo-TPE.

[47] Ding, Y.; Fusco, V.: Improved physical layer secure wireless communications using a directional modulation enhanced retrodirective array. General Assembly and Scientific Symposium (GASS), 2014 XXXIst URSI, 2014, doi: 10.1109/URSIGASS.2014.6929294

Bibliographies

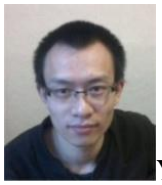

Yuan Ding received his Bachelor's degree from Beihang University (BUAA), Beijing, China, in 2004, received his Master's degree from Tsinghua University, Beijing, China, in 2007, and received his Ph.D. degree from Queen's University of Belfast, Belfast, UK, in 2014, all in Electronic Engineering.

He was a RF engineer in Motorola R&D centre (Beijing, China) from 2007 to 2009, before joining Freescale semiconductor Inc. (Beijing, China) as a RF field application engineer, responsible for high power base-station amplifier design, from 2009 to 2011. He is now a research fellow at the ECIT institute, Queen's University of Belfast, Belfast, United Kingdom. His research interests are in antenna array and physical layer security. He was the recipient of the IET Best Student Paper award at LAPC 2013 and the recipient of the Young Scientists Awards in General Assembly and Scientific Symposium (GASS), 2014 XXXIst URSI.

Vincent F. Fusco holds a personal chair in High Frequency Electronic Engineering at Queens University of Belfast. His research interests include active antenna and front-end MMIC techniques. He is head of the High Frequency Laboratories at QUB where he is also director of the International Centre for System on Chip for Advanced Microwireless. Professor Fusco has published over 450 scientific papers in major journals and in referred international conferences. He has authored two text books, holds patents related to self-tracking antennas and has contributed invited papers and book chapters. He serves on the technical programme committee for various international conferences including the European Microwave Conference. He is a Fellow of both the Institution of Engineering and Technology and the

Institute of Electrical and Electronic Engineers. In addition he is a Fellow of the Royal Academy of Engineers and a member of the Royal Irish Academy. In 2012 he was awarded the IET Senior Achievement Award the Mountbatten Medal.

List of figures and tables